PROCEEDINGS OF SCIENCE

Some results on excited hadrons in 2-flavor QCD

Georg P. Engel*
Institut für Physik, FB Theoretische Physik, Universität Graz, A–8010 Graz, Austria
E-mail: georg.engel@uni-graz.at

C. B. Lang
Institut für Physik, FB Theoretische Physik, Universität Graz, A–8010 Graz, Austria
E-mail: christian.lang@uni-graz.at

Markus Limmer
Institut für Physik, FB Theoretische Physik, Universität Graz, A–8010 Graz, Austria
E-mail: markus.limmer@uni-graz.at

Daniel Mohler
TRIUMF, 4004 Wesbrook Mall Vancouver, BC V6T 2A3, Canada
E-mail: mohler@triumf.ca

Andreas Schäfer
Institut für Theoretische Physik, Universität Regensburg, D–93040 Regensburg, Germany
E-mail: andreas.schaefer@physik.uni-regensburg.de

Results of hadron spectroscopy with two dynamical mass-degenerate chirally improved quarks are presented. Three ensembles with pion masses of $322(5)$, $470(4)$ and $525(7)$ MeV, lattices of size $16^3 \times 32$, and lattice spacings close to 0.15 fm are investigated. We discuss the possible appearance of scattering states, considering masses and eigenvectors. Partially quenched results in the scalar channel suggest the presence of a 2-particle state, however, in most channels we cannot identify them. Where available, we compare to results from quenched simulations using the same action.

The XXVIII International Symposium on Lattice Field Theory, Lattice2010
June 14-19, 2010
Villasimius, Italy

*Speaker.

1. Introduction

The majority of hadronic states in the Particle Data Group's collection are hadron excitations [1]. So far, lattice QCD provides the only known way to perform ab-initio calculations of the corresponding observables. This article is another step in this enterprise. We use the Chirally Improved (CI) Dirac operator [2], which is an approximate solution of the Ginsparg-Wilson (GW) equation [3]. We present results of ground states as well as excited states, making use of the variational method. In addition to the light quarks we also consider heavier valence (strange) quarks and include strange hadrons in our analysis. We discuss the possible appearance of scattering states and compare to quenched results using the same action. Preliminary results have been presented in [4]. A more complete discussion of the results is found in [5].

2. Simulation details

All details of the simulation method are given in [6]. The Chirally Improved Dirac operator (D_{CI}) is obtained by insertion of the most general ansatz for a Dirac operator into the GW equation and comparison of the coefficients. Furthermore, we include one level of stout smearing as part of the definition of D_{CI}, and use the Lüscher-Weisz gauge action. We generate the dynamical configurations with a Hybrid Monte-Carlo (HMC) algorithm. We simulate three ensembles with lattices of size $16^3 \times 32$, for details see Table 1. The variational method [7] is used to extract ground and excited states. Given a set of interpolators (with given quantum numbers) the corresponding correlation matrix is

$$C_{ij}(t) \;=\; \langle 0|O_i(t)O_j^\dagger|0\rangle = \sum_{k=1}^{N} \langle 0|O_i|k\rangle\langle k|O_j^\dagger|0\rangle\, \mathrm{e}^{-tE_k}. \tag{2.1}$$

In the variational method, the idea is to offer a basis of suitable interpolators, from which the system chooses the linear combinations closest to the physical eigenstates $|k\rangle$. The generalized eigenvalue equation

$$C(t)\,\vec{v}_k \;=\; \lambda_k(t,t_0)\,C(t_0)\,\vec{v}_k\,, \qquad \lambda_k(t,t_0) \propto \mathrm{e}^{-(t-t_0)\,E_k}\left(1+\mathcal{O}(\mathrm{e}^{-(t-t_0)\,\Delta E_k})\right)\,, \tag{2.2}$$

gives the energies of the eigenstates, where ΔE_k is the distance of E_k to the closest state. The corresponding eigenvectors represent the linear combinations of the given interpolators which are

set	β_{LW}	m_0	configs	a[fm]	m_π[MeV]	m_{AWI}[MeV]	L[fm]	$m_\pi L$
A	4.70	-0.050	100	0.151(2)	525(7)	43.0(4)	2.42(3)	6.4
B	4.65	-0.060	200	0.150(1)	470(4)	35.1(2)	2.40(2)	5.7
C	4.58	-0.077	200	0.144(1)	322(5)	15.0(4)	2.30(2)	3.7

Table 1: Bare parameters of the simulation: Three ensembles (A,B,C) at different gauge couplings β_{LW} and quark mass parameters m_0. The number of configurations, lattice spacing from the static potential assuming a Sommer parameter of $r_{0,exp} = 0.48$ fm, the pion mass, the (non-renormalized) AWI-mass, the lattice size and the dimensionless product of the pion mass with the physical lattice size are given. For more details see [6].

closest to the physical states considered. We use two Gaussian (narrow and wide) and derivative sources. The gaussian sources are computed using gauge-covariant Jacobi smearing, the derivative source are obtained by applying the covariant difference operators on the wide source. Combining these quark sources we construct several interpolators in each hadron channel in order to be able to extract excited states using the variational method. All sources are located in a single time slice and built on configurations which have been hypercubic-smeared (HYP) in the spatial directions three times. Tables of the interpolators are found in the Appendix of [5]. We consider isovector-mesons, which are free of disconnected diagrams. We use the meson interpolator construction as described in detail in [8], which is similar to constructions previously used in [9, 10, 11]. For the construction of baryon interpolators we use only Gaussian smeared quark sources.

In defining the lattice scale we use a mass-dependent scheme, since we have only one ensemble at each value of the gauge coupling. Nevertheless, we assume our path in parameter space to be close to the one in the mass-independent scheme, and expect that the analytic form of the chiral extrapolation should be similar, although with different expansion coefficients. Therefore, we perform chiral fits linear in the pion mass squared for all results.

3. Results

In all plots, filled symbols denote dynamical results and open symbols denote partially quenched results. The energy levels are obtained by a correlated exponential fit to the leading eigenvalues (2.2) in a range of t-values where we identify a plateau behaviour of effective mass and/or eigenvector components.

We discuss the possible appearance of scattering states considering masses, partially quenched data and eigenvectors. Neglecting the interactions of the hadronic bound states and finite volume effects, the energy level $E(A,B)$ for two free hadrons reads

$$E\left(A(\vec{p}),B(-\vec{p})\right) = \left(\sqrt{m_A^2+|\vec{p}|^2}+\sqrt{m_B^2+|\vec{p}|^2}\right)\left(1+\mathcal{O}(ap)\right) . \tag{3.1}$$

The symbols $\times$ and $+$ in the plots represent the tentative positions of expected energy levels of free particle scattering states according to (3.1). The corresponding non-correlated statistical uncertainty is of the magnitude of 5 to 60 MeV.

3.1 The 1^{--} channel: ρ

We find an excellent plateau for the ground state and an excited state signal compatible with experimental data (see Fig. 1). On the lattice, for our ensemble parameters the energy of the P wave scattering state $\pi\pi$ would be between the ρ ground state and the first excitation, but no such state is observed here. Comparing with quenched results using the same action [8] and taking into account the different Sommer parameter value used in the quenched analysis ($r_{0,exp} = 0.5$ fm), we find that the dynamical ρ ground state comes out significantly lighter than its quenched counterpart.

3.2 The 0^{++} channel: a_0

We find large effects due to partial quenching close to the dynamical point, especially at small pion masses (see Fig. 2). Our partially quenched data are well described by the partially quenched

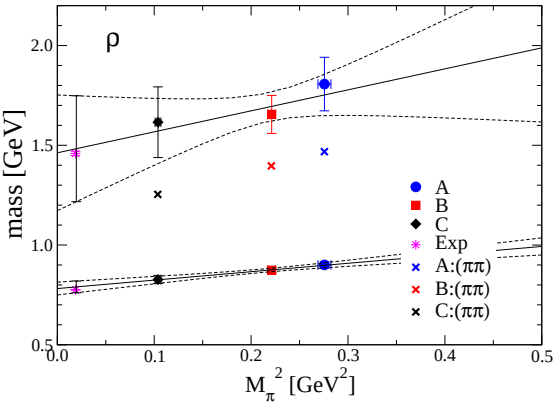

Figure 1: Mass plot for the 1^{--} channel (ρ), ground state and first excitation. The estimated energy level of the P wave scattering state $\pi\pi$ lies between the ground and the first excited state. The results suggest that the scattering state is not observed.

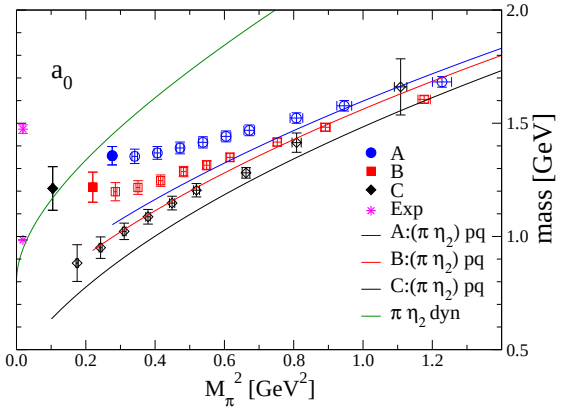

Figure 2: Mass plot for the 0^{++} channel (a_0). The blue, red and black curves (online version) show a prediction of the partially quenched ("pq") $\pi\eta_2$ for $m_{val} \gg m_{sea}$. The green curve (online version) shows an estimate of the dynamical ("dyn") $\pi\eta_2$ [5].

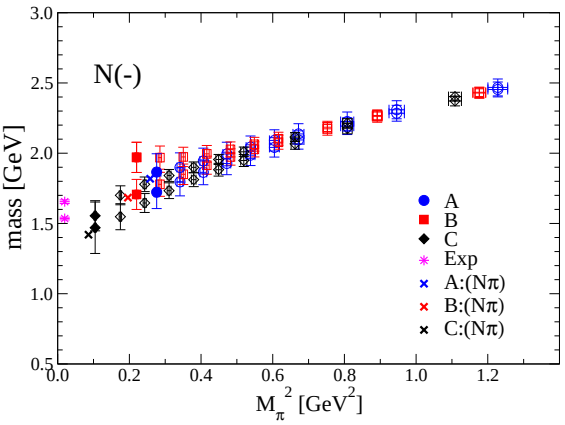

Figure 3: Mass plot for the nucleon negative parity channel. For clarity, we display the S wave scattering state πN slightly shifted to the left. The mass results (values below the ground state mass of N(1535)) suggest an interpretation in terms of level crossing, but the eigenvectors contradict this picture (see Fig. 5).Figure taken from [5].

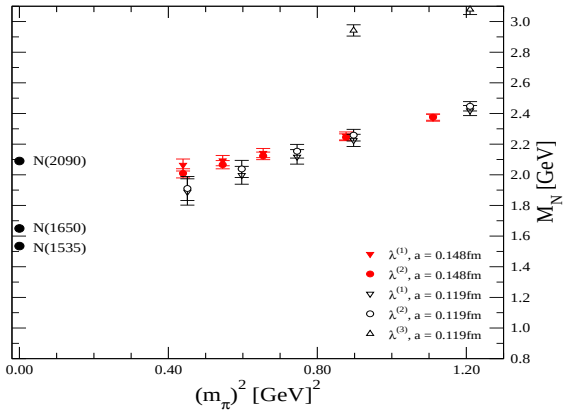

Figure 4: Mass plot for nucleon negative parity from quenched simulations using the same action. Data is only available for pion masses larger than 400 MeV, thus the bending down of dynamical data at small pion masses cannot be compared. Figure taken from [14].

formulae of the scattering state [12], and thus are interpreted as contributions of the 2-particle state $\pi\eta_2$. However, at the physical point, the particle content remains unclear. The ground state energy level in quenched simulations with the same action [8, 13] was extracted only at larger pion masses, being compatible with our dynamical data of set A, extrapolating to the $a_0(1450)$ rather than to $a_0(980)$. The spectroscopy of the light scalar channel appears to benefit from sea quarks.

3.3 Nucleon negative parity

The mass results suggest a large contribution of the S wave scattering state πN at small pion masses

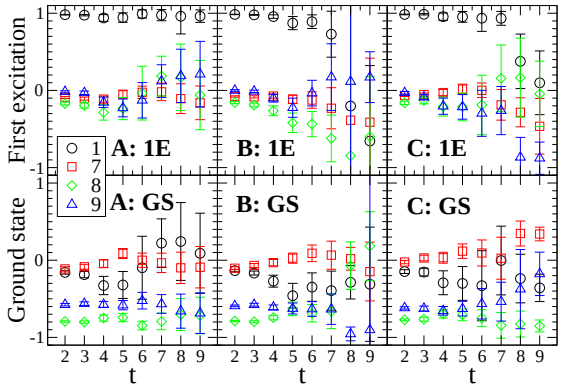

Figure 5: Eigenvectors of the nucleon negative parity channel, ground state and first excitation at the dynamical point. In all three ensembles the ground state is dominated by pseudoscalar, the first excitation by scalar diquark (similar to the quenched results in [14]). One may conclude that no level crossing of the lowest two states is observed. Plot taken from [5].

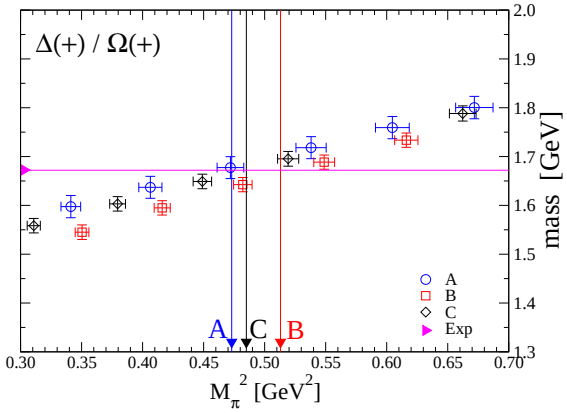

Figure 6: Extracting the strange quark mass parameter by identifying a partially quenched Δ with $\Omega(1670)$, represented by the magenta (online version) horizontal line. Crossing this line with the partially quenched Δ mass curves defines the bare strange quark mass parameter of A, B and C, illustrated by the three vertical lines [5].

and thus an interpretation in terms of a level crossing for pion masses in the range of 320 to 530 MeV (see Fig. 3). Unfortunately, the bending down of the dynamical data at small pion masses cannot be compared to results from quenched simulations using the same action, since they are only available for pion masses larger than 400 MeV (see Fig. 4). However, considering the eigenvectors, we find that in all three ensembles the ground state is dominated by the pseudoscalar diquark, the first excitation by the scalar diquark interpolator (see Fig. 5). Qualitatively, the eigenvectors of quenched simulations using the same action [14] show the same behavior. Since the argument based on the eigenvectors is assumed to be more reliable than the one based on the masses, we may conclude that no level crossing of the lowest two states is observed for pion masses in the range of 320 to 530 MeV and that both are mainly 1-particle states.

3.4 Setting the strange quark mass

We use our partially quenched results in the Δ positive parity channel to identify the strange quark mass parameters (see Fig. 6). Estimating the mass of the isoscalar ϕ from the results for ρ at strange quark mass values serves as a cross-check for the strange quark mass. The result fits the experimental $\phi(1020)$ nicely (see Fig. 7), indicating that our approach is consistent. The ground state levels of Σ and Ξ positive parity provide additional affirmative cross-checks [5].

3.5 Σ negative parity

In the Σ negative parity channel we find a ground state and two excitations (see Fig. 8). Similar to the nucleon negative parity channel, the results suggest an interpretation in terms of a level crossing of the 1- and 2-particle (KN) states. However, analogously to the nucleon negative parity channel, the eigenvectors do not support this picture.

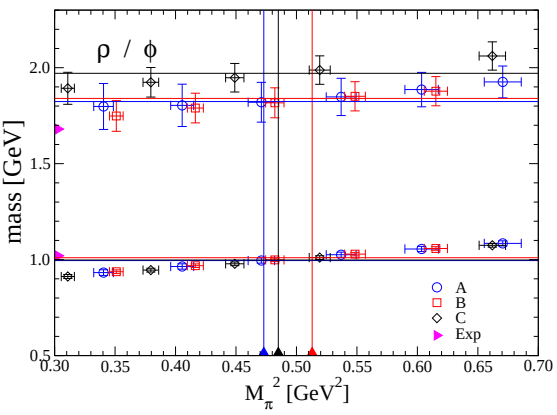

Figure 7: Cross-check of the obtained strange quark mass parameter: The partially quenched ϕ from the ground state of the 1^{--} channel fits the experimental $\phi(1020)$ very nicely. The result for the excited ϕ is higher than the experimental value, the deviation may be due to the neglected disconnected diagrams or simply due to the weak signal.

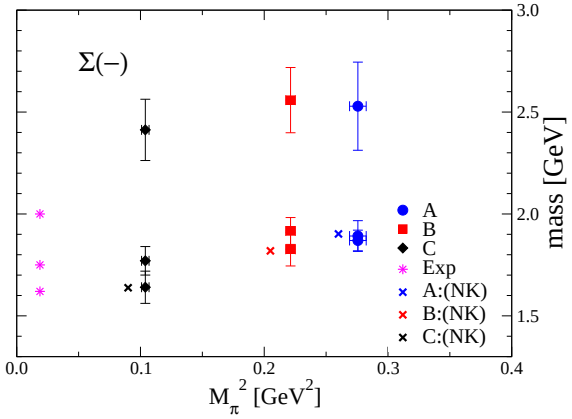

Figure 8: Mass plot for the Σ negative parity channel (dynamical data only). For better identification, we display the scattering states shifted to the left. The mass results suggest an interpretation in terms of a level crossing of the 1- and 2-particle (KN) states. However, analogously to the nucleon negative parity channel, the eigenvectors contradict this picture.

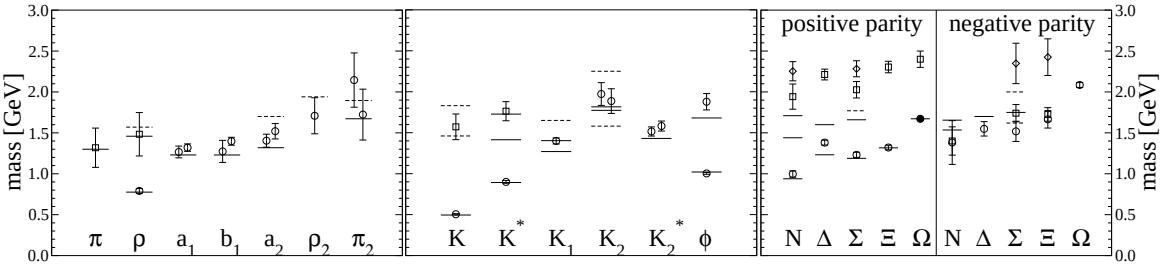

Figure 9: Mass results for light mesons, strange mesons and baryons (left to right), obtained by chiral extrapolation of dynamical light quarks linear in the pion mass squared. Experimental values listed by the Particle Data Group [1] are denoted by horizontal lines, the ones needing confirmation by dashed lines. Results shown aside each other are obtained using different sets of interpolators aiming for the same state. Strange quarks are implemented by partial quenching, the strange quark mass parameter is set using $\Omega(1670)$. Excited baryons seem to systematically suffer from finite volume effects. Figure taken from [5].

4. Conclusions

We presented results of hadron spectroscopy from three ensembles (pion masses from 320 to 530 MeV) using the Chirally Improved Dirac operator with two light sea quarks (see Fig. 9). The strange hadron spectrum was accessed using partially quenched strange quarks. We discussed the possible appearance of scattering states. The coupling of our interpolators to many-particle states seems to be weak and such states are barely, if at all, identifiable. Only in the light scalar channel the partially quenched data suggest a large contribution from an S channel 2-particle state of pseudoscalars. However, at the dynamical point no clear statement is possible. In the negative parity nucleon and Σ channels, the eigenvectors do not confirm the picture of the S wave 2-particle states, either, although such an admixture cannot be completely excluded. Comparison to quenched

simulations shows that the spectroscopy in the light scalar and light vector channels seems to benefit slightly from dynamical quarks. However, in most channels we did not observe a significant difference between quenched and dynamical simulations.

Acknowledgments

We thank C.R. Gattringer, L.Y. Glozman and S. Prelovsek for valuable discussions. The calculations have been performed on the SGI Altix 4700 of the Leibniz-Rechenzentrum Munich and on local clusters at ZID at the University of Graz. M.L. and D.M. have been supported by "Fonds zur Förderung der Wissenschaftlichen Forschung in Österreich" (DK W1203 -N08). D.M. acknowledges support by COSY-FFE Projekt 41821486 (COSY-105) and by Natural Sciences and Engineering Research Council of Canada (NSERC) and G.P.E., M.L. and A.S. acknowledge support by the DFG project SFB/TR-55.

References

[1] C. Amsler et al. (Particle Data Group), Phys. Lett. B **667**, 1 (2008).

[2] C. Gattringer, Phys. Rev. D **63**, 114501 (2001), hep-lat/0003005; C. Gattringer, I. Hip, C. B. Lang, Nucl. Phys. B **597**, 451 (2001), hep-lat/0007042.

[3] P. H. Ginsparg and K. G. Wilson, Phys. Rev. D **25**, 2649 (1982).

[4] G. Engel, C. Gattringer, C. B. Lang, M. Limmer, D. Mohler, and A. Schäfer, PoS **LAT09**, 088 (2009), arXiv:0910.2802.

[5] G. Engel, C. B. Lang, M. Limmer, D. Mohler, and A. Schäfer, Phys. Rev. D **82**, 034505 (2010), arXiv:1005.1748.

[6] C. Gattringer, C. Hagen, C. B. Lang, M. Limmer, D. Mohler, and A. Schäfer, Phys. Rev. D **79**, 054501 (2009), arXiv:0812.1681.

[7] C. Michael, Nucl. Phys. B **259**, 58 (1985); M. Lüscher and U. Wolff, Nucl. Phys. B **339**, 222 (1990).

[8] C. Gattringer, L. Y. Glozman, C. B. Lang, D. Mohler, and S. Prelovsek, Phys. Rev. D **78**, 034501 (2008), arXiv:0802.2020.

[9] P. Lacock, C. Michael, P. Boyle, and P. Rowland (UKQCD Collaboration), Phys. Rev. D **54**, 6997 (1996), hep-lat/9605025.

[10] X. Liao and T. Manke (2002), hep-lat/0210030.

[11] J. J. Dudek, R. G. Edwards, N. Mathur, and D. G. Richards, Phys. Rev. **77**, 034501 (2008), arXiv:0707.4162.

[12] S. Prelovsek, C. Dawson, T. Izubuchi, K. Orginos, and A. Soni, Phys. Rev. D **70**, 094503 (2004), hep-lat/0407037.

[13] T. Burch, C. Gattringer, L. Y. Glozman, C. Hagen, C. B. Lang, and A. Schäfer, Phys. Rev. D **73**, 094505 (2006), hep-lat/0601026.

[14] T. Burch, C. Gattringer, L. Y. Glozman, C. Hagen, D. Hierl, C. B. Lang, and A. Schäfer, Phys. Rev. D **74**, 014504 (2006), hep-lat/0604019.